Applied Physics Letters

RESEARCH ARTICLE | JUNE 12 2023

Nonlinear emission in $CsPbBr_3$ decorated metasurfaces

Giammarco Roini ; Gabriele Calusi ; Matteo Ferroni ; Nicoletta Granchi ; Ivano Alessandri ; Anna Vinattieri

Appl. Phys. Lett. 122, 241101 (2023)
https://doi.org/10.1063/5.0140471

Applied Physics Letters ARTICLE pubs.aip.org/aip/apl

Nonlinear emission in $CsPbBr_3$ decorated metasurfaces

Cite as: Appl. Phys. Lett. **122**, 241101 (2023); doi: 10.1063/5.0140471
Submitted: 28 December 2022 · Accepted: 24 May 2023 ·
Published Online: 12 June 2023

Giammarco Roini,[1] Gabriele Calusi,[2] Matteo Ferroni,[3,4,5] Nicoletta Granchi,[2,6] Ivano Alessandri,[1,5,7] and Anna Vinattieri[2,6,8,a)]

AFFILIATIONS

[1]Department of Information Engineering, University of Brescia, via Branze 38, Brescia, Italy
[2]Department of Physics and Astronomy, University of Florence, via G. Sansone 1, Sesto F.no, Italy
[3]Department of Civil Engineering, Architecture, Territory, Environment and Mathematics (DICATAM), University of Brescia, Via Branze 43, Brescia, Italy
[4]CNR-IMM Bologna, via Gobetti 101, Bologna 40129, Italy
[5]INO-CNR-UdR Brescia, via Branze 38, Brescia 25123, Italy
[6]LENS, via N.Carrara 1, Sesto F.no, Italy
[7]INSTM-UdR Brescia, via Branze 38, Brescia 25123, Italy
[8]INFN-Firenze, via G. Sansone 1, Sesto F.no, Italy

[a)]**Author to whom correspondence should be addressed:** anna.vinattieri@unifi.it

ABSTRACT

Halide perovskites are extremely interesting semiconductors for innovation in optoelectronics and photovoltaics. In particular, they are efficient emitters of both incoherent and coherent light and, therefore, of interest as active materials in lasers, light amplification systems (resonators and waveguides), and other photonic devices. Here, we present a set of experimental results concerning nonlinear effects in the radiative emission of $CsPbBr_3$ films deposited by spin-coating on a silicon substrate and on metasurfaces realized by microspheres having a core of SiO_2 and a shell of TiO_2 (*T-Rex*). We evidence the presence of *amplified spontaneous emission* which, depending on the sample structure, shows different behavior as a function of the excitation power. In particular, we distinguish between two processes: light amplification by randomly arranged emitters and amplification by a quite ordered distribution of nanocrystals around a resonator.

In the last decade, halide perovskites (HPs) have received considerable interest from the communities of physicists, chemists, and materials scientists for the many possible applications to replace the classic semiconductors for photovoltaics, optoelectronics, sensors, and nonlinear photonics.[1–3] An important advantage of these materials is the ease/low cost in the material synthesis/deposition and the possibility of engineering the bandgap by appropriately choosing the constituent elements and their respective concentrations. In particular, inorganic HP retains the excellent properties of organic HP as the high mobility of the charge carriers, the high absorption coefficient being direct bandgap semiconductors, and the small cross section of the defects (mainly halogen vacancies),[4] showing a better stability and longer lifetime for both shelf storage and under illumination and exposure in ambient conditions.[5] Therefore, they are substituting organic HP for applications in optoelectronics and photonics. Among inorganic HP, $CsPbX_3$ (X = Cl, Br, I) is deeply investigated because the bandgap energy E_g can be finely tuned to cover the whole visible range, when alloying different halides.[6]

Recently, a significant research effort has been directed to the control and manipulation of the light properties by embedding/decorating photonic structures and metasurfaces with halide perovskites nanocrystals for efficient emitters with controlled properties as polarization, directionality, etc.[7,8] In particular, the evidence of amplified spontaneous emission (ASE) represents the ground for the realization of innovative laser sources.[9] Here, we present an experimental investigation concerning the observation of nonlinear emission in metasurfaces decorated with $CsPbBr_3$ nanocrystals with characteristics that are typical of ASE. Depending on the specific morphology of the

surface where $CsPbBr_3$ is deposited, we find different behavior of the ASE signal with transition from a *random* lasing behavior to a *few modes* lasing.

Samples were prepared depositing on a Si substrate SiO_2 spheres of different diameters and then covering with a 100 nm TiO_2 layer by atomic layer deposition (ALD). In this way, the TiO_2 layer covers the substrate and surrounds the spheres leading to core–shell beads called *T-Rex*.[10] The TiO_2 layer has several beneficial effects: besides fixing the sphere position so to improve the mechanical stability of the sample, also it fills the interstices between the spheres strongly enhancing the optical coupling between them. As shown for short chains of microspheres, the efficient coupling of the whispering gallery modes between adjacent spheres requires a very precise control of their relative distance that is difficult to get on extended samples.[11] The deposition of the TiO_2 layer allows to overcome the related problems so to realize an extended array of optically connected spheres where the whispering gallery mode can propagate.[12,13] In addition, the coverage of the SiO_2 sphere with an high refraction index layer (2.5 for TiO_2) modifies the mode spatial profile enhancing the e.m. field near the surface[14] and then increasing the photonic coupling to the outer material. In fact, *T-Rex* has been demonstrated to provide a substantial sensitivity enhancement in surface enhanced Raman scattering (SERS) experiments without the use of plasmons.[15,16]

An hexagonal 2D lattice of spheres is formed on the substrate (see S1 in the supplementary material), constituting the metasurface which is then decorated by spinning the $CsPbBr_3$ solution. After the solvent evaporation, micro/nanocrystals are formed. Samples with different *T-Rex* microsphere diameter were realized: in this paper, we present results on metasurfaces with 2 μm (sample A) and 6 μm (sample B) *T-Rex* diameter; a sample where $CsPbBr_3$ was deposited directly on the TiO_2 layer on Si (sample C) is also shown for comparison. Details concerning the $CsPbBr_3$ preparation are reported in the supplementary material.

In Figs. 1(a) and 1(b), typical SEM images for samples A and B are reported, showing the presence of sub-micrometer-sized crystals of $CsPbBr_3$. From the SEM images, we can observe that perovskite

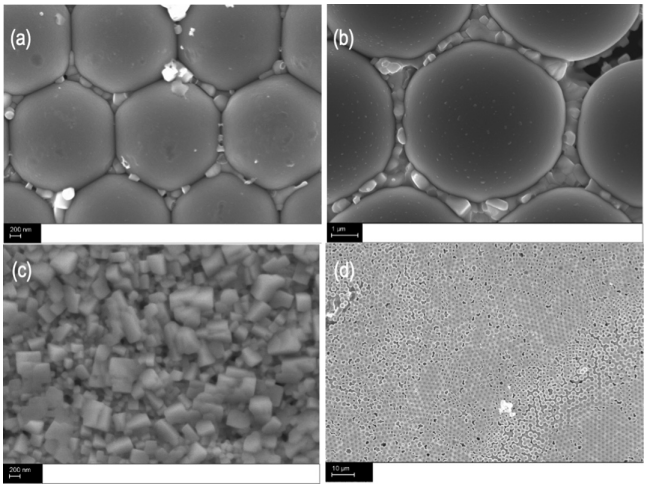

FIG. 1. SEM images of sample A (a), sample B (b), and sample C (c). SEM image of a large portion of sample A (d).

mainly crystallizes between the *T-Rex* spheres. A SEM image of a large area of sample A [Fig. 1(d)] shows the arrangement of the *T-Rex* spheres on the substrate. It is worth noting that most of the reports dealing with halide perovskite nanocrystals or quantum dots bound to microresonators[17,18] focuses on the study of a single resonator while in our case we have the possibility to investigate a regular assembly of resonators in a macro-sized area. If we observe the morphology of sample C in which the perovskite is deposited directly on the TiO_2 layer which covers the silicon substrate, without the presence of the *T-Rex* spheres [Fig. 1(c)], the $CsPbBr_3$ film is more compact with a density of microcrystals at least one order of magnitude higher respect to samples A and B. Moreover, the $CsPbBr_3$ crystal size in sample C is greater respect to what found in samples A and B. Therefore, it turns out that, despite the same procedure used in the spin-coating deposition, the presence of the spheres modifies the perovskite assembly. It is also worth noting that in samples A and B the microcrystals are confined in the interstices between the spheres, filled by TiO_2, and no crystal formation occurs under them. However, the distribution of microcrystals in samples A and B is not homogeneous: in some regions, crystals completely fill the interstices, in other regions, less amount of them is present between the spheres.

In order to provide a room temperature optical characterization of the samples, we performed photoluminescence (PL) experiment with a scanning near-field optical microscope (SNOM) in illumination/collection configuration and a home-made confocal microscope (hereafter indicated as *micro-PL*). Details of the SNOM and *micro-PL* are reported in the supplementary material. The comparison of the SNOM topography map and the corresponding SNOM PL map detected at the PL peak energy (S2 in the supplementary material) confirms that in sample A, PL mostly comes from the side regions of the spheres. However, the size of the *T-Rex* limits the possibility of using SNOM when the bead diameter is >2 μm.

In order to highlight the morphology of the samples in a wider region, we used the micro-PL setup. In Fig. 2, the room temperature PL image of sample B as detected by a CCD camera with a low-pass filter at 500 nm is reported after excitation of a wide sample region [Fig. 2(a)], using the microscope only in collection mode; in Fig. 2(b), we excite and collect the PL through the microscope having a 5 μm excitation spot (limits are due to laser diode beam quality). It is evident that the beads network with the perovskite crystals between the spheres (in the dark) and, as shown in Fig. 2(b), the strong PL light diffusion, indicating an efficient coupling between the spheres and the nanocrystals. In the supplementary material (S3), the laser spot is superposed to a *micro-PL* image of samples B in a different region of the sample, so to highlight the PL light diffusion. A similar image for sample A is also reported in the supplementary material.

PL spectra at the macro-scale allowed us to explore different excitation conditions (CW or pulsed excitation, temperature, and excitation power). All details of the experimental setups are reported in the supplementary material.

First of all, we present PL spectra after CW excitation at 450 nm (2.76 eV), then comparing them with the results obtained by exciting the samples with 300 ps pulses at 266 nm (4.66 eV). It is worth noting that in both cases a significant excess of energy with respect to the bandgap energy (2.3 eV) is provided to the carriers.

In Fig. 3, low temperature PL spectra are shown varying the excitation power at 450 nm in the range 0.5–1 mW for samples A and C.

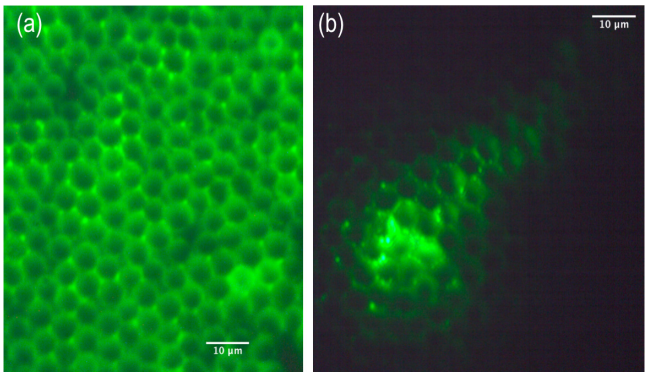

FIG. 2. (a) Micro PL image of sample B after excitation of a large spot on the sample with a 355 nm laser. The image is collected filtering the PL with a low pass filter at 500 nm. (b) Micro PL image of sample B after excitation of a micrometer-sized spot on the sample with a 405 nm laser. The image is collected filtering the PL with a low pass filter at 500 nm.

Sample C [Fig. 3(b)] shows an emission peak at 2.293 eV coming from the exciton recombination of micrometer-sized crystals and the PL full width half maximum (FWHM) is 18 meV in agreement with literature results for spin-coated samples.[19] Moreover, a minor contribution to PL comes from a an higher energy shoulder at 2.32 eV possibly due to excitonic recombination from $CsPbBr_3$ nano-sized crystals.[20] Sample A shows a PL peaked between 2.302 and 2.308 eV depending on the position of the excitation spot and the FWHM varies between 20 and 22 meV [Fig. 3(a)]. A different strain condition could be responsible of the PL blue energy shift respect to sample C; however, similar spread of values are commonly found in the literature.[19,21] Quite remarkable is the similar value of the PL intensity when comparing samples A and C at the same excitation density. In fact, if we provide an estimate of the volume of excited halide perovskite in the two different samples considering that in sample A (B) we can only fill the interstices, we would expect that the PL intensity of sample A (B) was at least an order of magnitude lower than sample C. It is worth noting that perovskite is only present around the spheres being the substrate and the SiO_2 spheres covered by the TiO_2 layer. Moreover, we cannot ascribe such finding to sample inhomogeneity which at maximum can account for a factor 2. Therefore, as we will show with simulation, this result indicates that the metasurface structure helps in the extraction of light from the sample.

When the PL spectra for different excitation power are normalized to the maximum of the emission [Fig. 3(c)], it turns out that the line shape remains the same except for the low energy tail which shows a sublinear trend increasing the excitation intensity. In Fig. 3(d), the PL spectrally integrated intensity as a function of the power P_{exc} is reported for the different samples along with the fit with a power law,

$$I_{PL} \sim P_{exc}^{\alpha}. \quad (1)$$

The α coefficient is between 1 and 1.1 for all the samples, indicating a linear dependence of the PL over four orders of magnitude in a generally speaking low excitation condition.

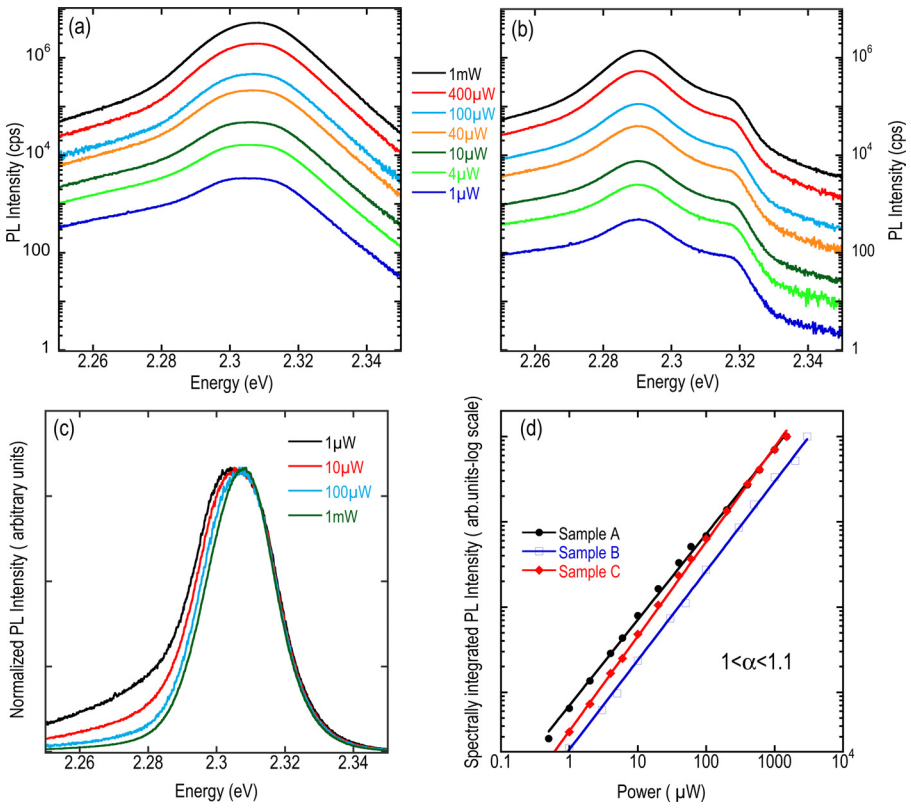

FIG. 3. PL spectra at 10 K as a function of the power under CW excitation in log scale (a) sample A, (b) sample C, (c) normalized PL spectra of sample A for different excitation power, and (d) dependence of the spectrally integrated PL on the excitation power for samples A, B, and C. The solid line is a fit with a power law and α is the power law exponent.

A different scenario is found when the excitation occurs by the 300 ps long pulses as shown in Fig. 4 for a temperature of 10 K.

For all samples, when the average power is $\geq$ 1mW, corresponding to pulse energy $\geq$ 50 nJ, narrow peaks appear (hereafter indicated as *modal* structure), at the limit of the setup resolution, and the emission increases superlinearly. The observed phenomenology is similar to what is reported in the literature relating to the establishment of an ASE and/or random lasing regime.[9,22,23] However, as we will show in the following, marked differences are found when we compare samples A and B where spheres are present, with sample C where spheres are absent. Increasing the lattice temperature, the presence of the *modal* structure persists up to $\approx$ 150 K as shown in Fig. 4(d). Above 150 K, the spectrum is smooth with no relevant feature. Moreover, a marked quenching of the PL is found. We observe that in the explored temperature range perovskite microcrystals maintain the orthorhombic phase,[24] and therefore, the observed effects cannot be ascribed to a phase change which occurs at 350 K. The blue shift of the emission with the increase in temperature is in agreement with the variation of the bandgap energy of $CsPbBr_3$.

If we acquire the PL spectra at 10 K, in the region where modes are present, in a kinetic mode, with a short time of exposure (21 ms) repeating the sequence with a time delay, we find that the modal structure is stable in the case of sample A while it changes in sample C (S4 in the supplementary material); this result suggests that the presence of the *T-Rex* beads plays a role in stabilizing in time each mode. If we focus on the low temperature spectra, having the photoluminescence a linear trend with the excitation power, to highlight the presence of nonlinear effects, it is advisable to subtract the lowest power spectra (0.5 mW) from each spectrum after having multiplied it by the appropriate factor to take into account the power value. This procedure removes the linear component of the emission, providing information on the remaining contribution, hereafter indicated as nonlinear contribution. The results are shown in Fig. 5 for sample C, which shows a superlinear increase in the emission with several modes as indicated in Fig. 5(b) and as expected for the ASE contribution. The solid line in the figure is a fit of the nonlinear contribution according to a power law with β as exponent. It turns out that the results for sample C [Fig. 6(b)] indicates the presence of ASE with a significant superlinearity even though in our experimental conditions the excitation energy is pretty low (at maximum 0.5 mJ/cm^2 per pulse).

In the case of sample A, increasing the excitation power, we find a slight thermal shift ($\approx$ 5 meV) that has to be taken into account for a proper analysis of the data. In Fig. 6(a), two spectra at 10 K are compared in log scale to evidence the low energy side sublinear behavior. In Fig. 6(b), the whole set of spectra is shown after the correction for the thermal shift. For a better reading, the abscissa-axis reports the energy after subtraction of the PL peak energy. Several narrow modes are present with a peculiar behavior on the excitation power. If we focus on three of them (P1, P2, and P3) and we report the corresponding intensity after the PL contribution subtraction we find the trend reported in Fig. 6(c).

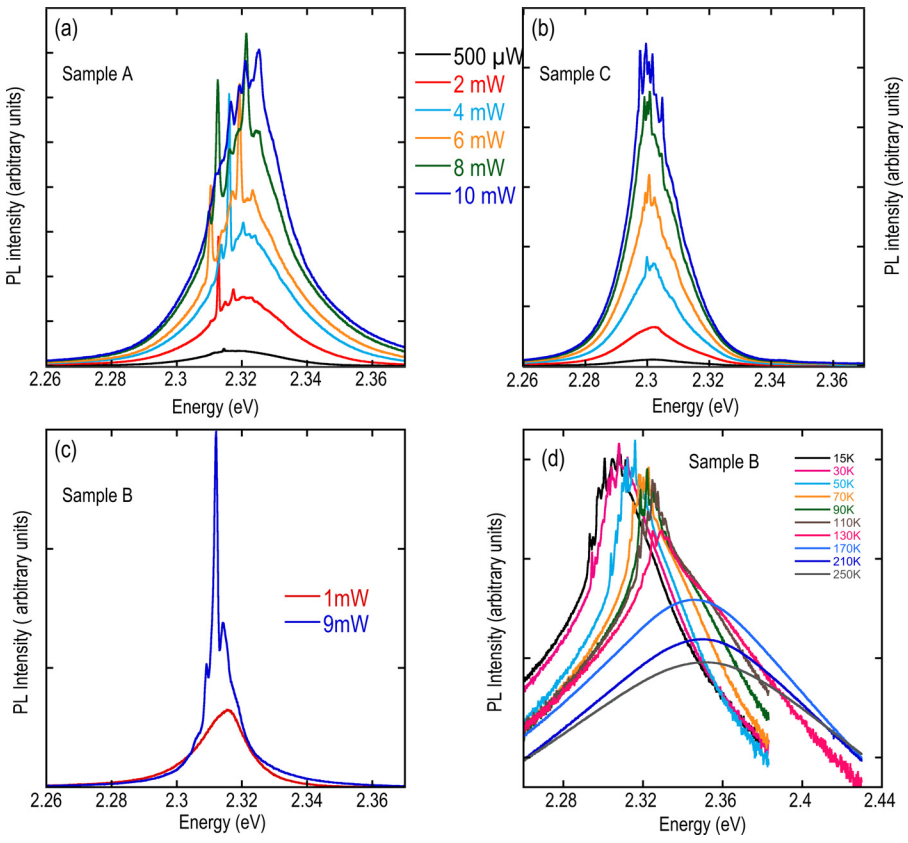

FIG. 4. PL spectra after excitation with pulses at 266 nm at 10 K: sample A (a), sample C (b), and sample B (c). Temperature dependence of PL for sample B (d).

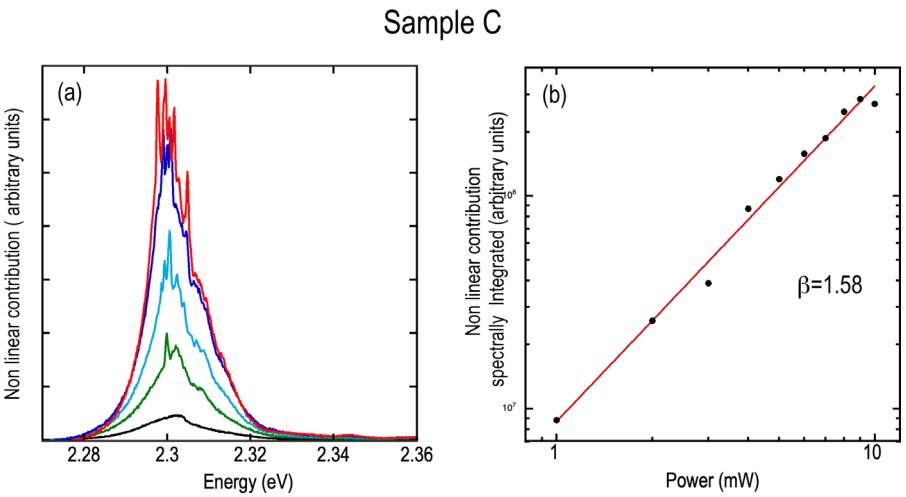

FIG. 5. Nonlinear contribution at 10 K extracted from spectra of Fig. 4 for sample C (a). Spectrally integrated nonlinear contribution as from (a) and the solid line corresponds to a power law fit with β indicated in the figure.

The most significant findings for sample A are: each mode presents a different threshold and the superlinear increase is followed by a saturation and a decrease. Only the lowest energy mode (14 meV on the low energy side) does not show saturation in the investigated excitation power range. It has to be noted that the PL remains linearly dependent on the excitation power as shown in Fig. 6(c). Similar results are shown in S5 in the supplementary material for sample B. We believe that the absence of a significant superlinear trend for samples A and B comes from the limited number of emitters present in the excited spot as indicated from the SEM images; the decrease observed for further increase in the excitation power could be possibly related to a local heating. Moreover, the mode stability in time as from S4 in the supplementary material suggests a transition from a random lasing behavior to a lasing related to the extended ensemble of coupled microresonators consisting of the *T-Rex* layer. An estimate of the Q-factor provides values between 2300 and 3300 depending on the considered mode. Quite remarkable it is also the persistence of the nonlinear emission up to 150 K, despite the low pulse energy used in the experiment. Recent literature data show the observation of ASE up to 300 K in compact films of $CsPbBr_3$ after a heat treatment[25] that leads to a re-crystallization with crystals of micrometric size bigger than those of the samples studied here. Therefore, the results here presented, where no post-growth treatment was used, seem promising, in particular, with regard to the integration of perovskite in the metasurface of *T-Rex*. It is also worth noting that the experiments were realized in a quasi-back-scattering geometry while most of the reports concerning the detection of ASE in halide perovskite samples were realized in a guided mode configuration:[26,27] this is a further evidence of the beneficial action of the metasurface in this case.

In order to theoretically verify the presence of enhancement in the perovskite emission in the presence of the *T-Rex* spheres (samples A and B) with respect to the flat substrate case (sample C) we performed finite difference time domain (FDTD) simulations, employing the commercial software Lumerical. To simulate the emission from

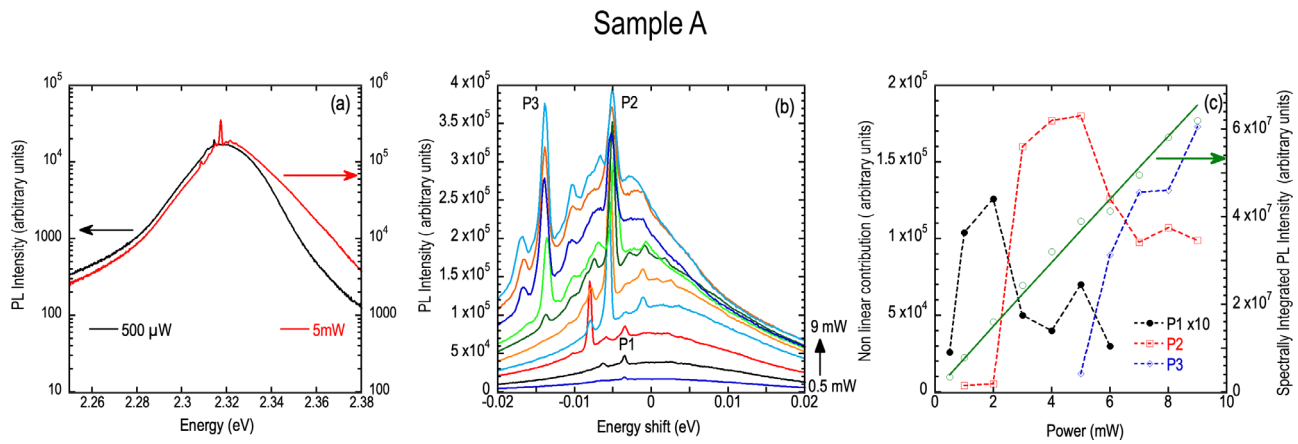

FIG. 6. (a) PL spectra for two different excitation powers to show the low energy side saturation. (b) PL spectra as a function of the excitation power corrected for the slight thermal shift. The abscissa-axis represents the energy shift respect to the PL peak energy. Three modes are evidenced (P1, P2, and P3). (c) Nonlinear contribution at energies of P1, P2, and P3 as a function of the excitation power. Dashed lines are guides for eye. The empty green dots represent the spectrally integrated PL intensity: the green solid line is a fit with a power law with exponent equal to 0.98.

the perovskite, a spectrally narrow electric dipole x-polarized is used, centered around 2.34 eV (no changes are found when the energy is in the range 2.3–2.36 eV) with a pulse length of 100 fs.

In Fig. 7(a), the simulation conditions are reported, where different materials are highlighted with different colors: to simulate the emission of sample C, the dipole is positioned on the substrate composed of a Si bulk and 100 nm thick layer of TiO_2. Then, the same dipole is positioned on top of a core–shell sphere with a diameter d = 2 μm (sample A) and d = 6 μm (sample B). In all cases, the intensity spectra are collected from a time monitor positioned at a distance of 400 nm from the dipole, and results are shown in Fig. 7(b). A clear enhancement of the electromagnetic field intensity in both samples A and B (blue and orange lines) is found with respect to the flat case. The maximum enhancement factor (4.5) is achieved for the bigger sphere, i.e., sample B. This simulation has to be considered a proof of principle test; in fact, in the experimental conditions, we always study a macroscopic region of the metasurface where a hexagonal assembly of spheres with dipoles is present. Simulations reported in the supplementary material (S6) evidence the presence of MIE resonances in the spheres in the spectral region where $CsPbBr_3$ emits. Recent reports[17,18,26,28,29] indicate lasing from multiple gallery-whispering of single microresonators decorated with $CsPbBr_3$ quantum dots or nanocrystals. Our results suggest that lasing can eventually occur from the coupling of the hexagonal arrangement of microspheres: in the supplementary material (S7) preliminary analysis is shown to verify this coupling condition.

In conclusion, we reported on the nonlinear emission in $CsPbBr_3$ films made by spin-coating on a semiconductor substrate and on a metasurface. Different morphology of the films is found depending on the presence/absence of the metasurface realized with *T-Rex* beads. Experimental results suggest that the presence of the *T-Rex* provides a better light extraction, as indicated by FDTD simulations on a single sphere. Measurements by varying the laser power showed a transition from a linear photoluminescence regime to a superlinear one with the appearance of modal structures in the spectral region of the maximum of the PL. While in the sample without the metasurface the phenomenology can be attributed to random lasing regime, the results found for the modal structures in samples with the beads suggests that coupled spherical microresonators promote a real lasing action as suggested by the Kinetic PL series. The results show that the realized metasurface provides in a simple way an ensemble of coupled microresonators suitable for enhancing the light–matter interaction, in principle, with any kind of nanoparticles. Additional improvements of the enhancement factor are expected optimizing the microsphere size with respect to the radiation wavelength.

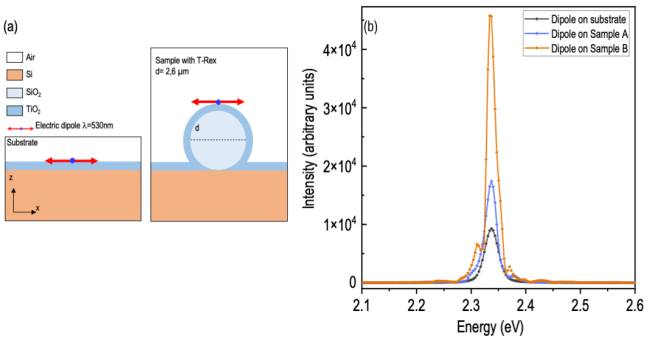

FIG. 7. (a) Sketch of the models simulated via FDTD method, respectively, representing the electric dipole on the substrate, the electric dipole on top of a core–shell sphere with diameter d (d = 2 μm sample A and d = 6 μm sample B). The sketches are not in scale. (b) FDTD intensity spectra for the three different scenarios corresponding to the panels of (a) showing the enhancement factor in the presence of the spheres.

See the supplementary material for details on sample preparation, experimental setups, additional information concerning experimental results, and simulation.

A.V. and G.R. acknowledge F. Bogani for critical reading and comments and A. Ristori for preliminary simulations.

AUTHOR DECLARATIONS

Conflict of Interest

The authors have no conflicts to disclose.

Author Contributions

Giammarco Roini: Formal analysis (equal); Investigation (equal); Writing – original draft (equal). **Gabriele Calusi:** Investigation (supporting). **Matteo Ferroni:** Investigation (equal). **Nicoletta Granchi:** Investigation (equal). **Ivano Alessandri:** Conceptualization (equal); Funding acquisition (equal); Writing – review & editing (equal). **Anna Vinattieri:** Conceptualization (equal); Funding acquisition (equal); Investigation (equal); Methodology (equal); Supervision (equal); Writing – original draft (equal); Writing – review & editing (equal).

DATA AVAILABILITY

The data that support the findings of this study are available from the corresponding author upon reasonable request.

REFERENCES

[1]A. K. Jena, A. Kulkarni, and T. Miyasaka, "Halide perovskite photovoltaics: Background, status, and future prospects," Chem. Rev. **119**, 3036–3103 (2019).
[2]Y. Fu, H. Zhu, J. Chen, M. P. Hautzinger, X.-Y. Zhu, and S. Jin, "Metal halide perovskite nanostructures for optoelectronic applications and the study of physical properties," Nat. Rev. Mater. **4**, 169 (2019).
[3]A. Ferrando, J. P. Martinez Pastor, and I. Suarez, "Toward metal halide perovskite nonlinear photonics," J. Phys. Chem. Lett. **9**, 5612–5623 (2018). pMID: 30180577.
[4]S. G. Motti, D. Meggiolaro, S. Martani, R. Sorrentino, A. J. Barker, F. De Angelis, and A. Petrozza, "Defect activity in lead halide perovskites," Adv. Mater. **31**, 1901183 (2019).
[5]W. Xiang, S. F. Liu, and W. Tress, "A review on the stability of inorganic metal halide perovskites: Challenges and opportunities for stable solar cells," Energy Environ. Sci. **14**, 2090–2113 (2021).
[6]L. Protesescu, S. Yakunin, M. I. Bodnarchuk, F. Krieg, R. Caputo, C. H. Hendon, R. X. Yang, A. Walsh, and M. V. Kovalenko, "Nanocrystals of cesium lead halide perovskites ($CsPbX_3$, X = Cl, Br, and I): Novel optoelectronic materials showing bright emission with wide color gamut," Nano Lett. **15**, 3692–3696 (2015).
[7]G. Adamo, J. Tian, H. N. S. Krishnamoorthy, D. Cortecchia, G. Long, and C. Soci, "Perovskite metamaterials and metasurfaces," in *Halide Perovskites for Photonics*, edited by A. Vinattieri and G. Giorgi (AIP Publishing, New York, 2021).

[8]K. Baryshnikova, D. Gets, T. Liashenko, A. Pushkarev, I. Mukhin, Y. Kivshar, and S. Makarov, "Broadband antireflection with halide perovskite metasurfaces," Laser Photonics Rev. **14**, 2000338 (2020).
[9]I. Suárez and J. P. M. Pastor, "Amplified spontaneous emission generation in lead halide perovskite semiconductors," in *Halide Perovskites for Photonics*, edited by A. Vinattieri and G. Giorgi (AIP Publishing, New York, 2021).
[10]I. Vassalini, O. Sisman, E. Comini, and I. Alessandri, "The role of morphology in all-dielectric sers: A comparison between conformal (*T-Rex*) and non conformal TiO_2 shells," Vib. Spectrosc. **109**, 103085 (2020).
[11]S. Kreps, V. Shuvayev, M. Douvidzon, B. Bathish, T. L. Abudi, A. Ghaznavi, J. Xu, Y. Lin, L. Deych, and T. Carmon, "Coupled spherical-cavities," AIP Adv. **12**, 125022 (2022).
[12]A. Yariv, Y. Xu, R. K. Lee, and A. Scherer, "Coupled-resonator optical waveguide:? A proposal and analysis," Opt. Lett. **24**, 711–713 (1999).
[13]Z. Chen, A. Taflove, and V. Backman, "Highly efficient optical coupling and transport phenomena in chains of dielectric microspheres," Opt. Lett. **31**, 389–391 (2006).
[14]I. Teraoka and S. Arnold, "Enhancing the sensitivity of a whispering-gallery mode microsphere sensor by a high-refractive-index surface layer," J. Opt. Soc. Am. B **23**, 1434–1441 (2006).
[15]I. Alessandri, "Enhancing Raman scattering without plasmons: Unprecedented sensitivity achieved by TiO_2 shell-based resonators," J. Am. Chem. Soc. **135**, 5541–5544 (2013).
[16]N. Bontempi, L. Carletti, C. De Angelis, and I. Alessandri, "Plasmon-free SERS detection of environmental Co_2 on TiO_2 surfaces," Nanoscale **8**, 3226–3231 (2016).
[17]M. B. Price, K. Lewellen, J. Hardy, S. M. Lockwood, C. Zemke-Smith, I. Wagner, M. Gao, J. Grand, K. Chen, J. M. Hodgkiss, E. Le Ru, and N. J. L. K. Davis, "Whispering-gallery mode lasing in perovskite nanocrystals chemically bound to silicon dioxide microspheres," J. Phys. Chem. Lett. **11**, 7009–7014 (2020).
[18]D. Yan, T. Shi, Z. Zang, S. Zhao, J. Du, and Y. Leng, "Stable and low-threshold whispering-gallery-mode lasing from modified $CsPbBr_3$ perovskite quantum dots@SiO_2 sphere," Chem. Eng. J. **401**, 126066 (2020).
[19]C. Wolf and T.-W. Lee, "Exciton and lattice dynamics in low-temperature processable $CsPbBr_3$ thin-films," Mater. Today Energy **7**, 199–207 (2018).
[20]N. Falsini, A. Ristori, F. Biccari, N. Calisi, G. Roini, P. Scardi, S. Caporali, and A. Vinattieri, "A new route for caesium lead halide perovskite deposition," J. Eur. Opt. Soc.-Rapid Publ. **17**, 8 (2021).
[21]F. Pan, J. Li, X. Ma, Y. Nie, B. Liu, and H. Ye, "Free and self-trapped exciton emission in perovskite $CsPbBr_3$ microcrystals," RSC Adv. **12**, 1035–1042 (2022).
[22]F. Biccari, A. Ristori, F. Gabelloni, C. Francioni, F. La China, N. Caselli, F. Intonti, M. Gurioli, J. Lee, S. Leblebici, A. Weber-Bargioni, and A. Vinattieri, "Superlinear emission in bare perovskite: Amplified spontaneous emission in disordered film versus single crystal lasing," Mater. Today: Proc. **4**, S12–S18 (2017).
[23]H. Zhang, L. Yuan, Y. Chen, Y. Zhang, Y. Yu, X. Liang, W. Xiang, and T. Wang, "Amplified spontaneous emission and random lasing using $CsPbBr_3$ quantum dot glass through controlling crystallization," Chem. Commun. **56**, 2853–2856 (2020).
[24]S. Svirskas, S. Balciunas, M. Simenas, G. Usevicius, M. Kinka, M. Velička, D. Kubicki, M. E. Castillo, A. Karabanov, V. V. Shvartsman, M. de Rosario Soares, V. Sablinskas, A. N. Salak, D. C. Lupascu, and J. Banys, "Phase transitions, screening and dielectric response of $CsPbBr_3$," J. Mater. Chem. A **8**, 14015–14022 (2020).
[25]N. Pourdavoud, T. Haeger, A. Mayer, P. J. Cegielski, A. L. Giesecke, R. Heiderhoff, S. Olthof, S. Zaefferer, I. Shutsko, A. Henkel, D. Becker-Koch, M. Stein, M. Cehovski, O. Charfi, H.-H. Johannes, D. Rogalla, M. C. Lemme, M. Koch, Y. Vaynzof, K. Meerholz, W. Kowalsky, H.-C. Scheer, P. Gorrn, and T. Riedl, "Room-temperature stimulated emission and lasing in recrystallized cesium lead bromide perovskite thin films," Adv. Mater. **31**, 1903717 (2019).
[26]S. Yakunin, L. Protesescu, F. Krieg, M. I. Bodnarchuk, G. Nedelcu, M. Humer, G. De Luca, M. Fiebig, W. Heiss, and M. V. Kovalenko, "Low-threshold amplified spontaneous emission and lasing from colloidal nanocrystals of caesium lead halide perovskites," Nat. Commun. **6**, 8056 (2015).
[27]M. L. De Giorgi, F. Krieg, M. V. Kovalenko, and M. Anni, "Amplified spontaneous emission threshold reduction and operational stability improvement in $CsPbBr_3$ nanocrystals films by hydrophobic functionalization of the substrate," Sci. Rep. **9**, 17964 (2019).
[28]H. Yu, X. Su, Y. Pan, D. Gao, J. Wang, R. Chen, J. Zhang, F. Dou, X. Zhang, K. Ge, X. Shi, T. Zhai, and L. Wang, "Narrow linewidth $CsPbBr_3$ perovskite quantum dots microsphere lasers," Opt. Mater. **133**, 112907 (2022).
[29]M. Xie, W. Gong, L. Kong, Y. Liu, Y. Mi, H. Guo, and S.-N. Luo, "Solution-processed whispering-gallery-mode microsphere lasers based on colloidal $CsPbBr_3$ perovskite nanocrystals," Nanotechnology **33**, 115204 (2022).